A New Design Method for the Clawpole Transverse Flux Machine. Application to the Machine No-Load Flux optimization. Part II: Optimization Aspects.

Nicolas Dehlinger, *Student Member, IEEE,* Maxime R. Dubois, *Member, IEEE*

***Abstract* -- This paper addresses the difficulty of modeling and optimizing transverse flux machines (TFMs). 3D flux line patterns, complex leakage paths and saturation of the magnetic material significantly add to the complexity of building accurate magnetic models to optimize TFMs. In this paper, a new design method is presented and applied to maximize the no-load flux of a Clawpole TFM. An error compensation mechanism combined to an analytical reluctance model is proposed as a solution to overcome inherent inaccuracies of TFM analytical models in a design process. As a natural complement to a previous communication focused the model and the error compensation mechanism, this paper investigates the use of this design method in an optimization context.**

***Index Terms*-- Modeling, Optimization, Finite Element Methods, Transverse Flux Machine.**

I. Introduction

The high torque and power capabilities of Transverse Flux Machines (TFMs) have been discussed in a number of publications [1]-[10]. These capabilities make TFMs an attractive solution in some low-speed, high torque applications such as direct-drive wind turbines or automotive electric traction [2]. Since its introduction by Weh in 1986 [1], several structures have been proposed with the transverse flux concept such as single- or double-sided machines, TFMs with surface magnets or with flux concentration [2].

This paper deals with the development of a new design method for TFMs. It is applied to the Clawpole TFM (CTFM) structure while it is not restricted to this particular TFM geometry. CTFM magnetic circuits are usually made from soft magnetic composite materials (SMC) for their isotropic properties and for manufacturing purposes. CTFMs offer a great compromise between torque density and ease of construction and manufacturing [3]-[5]. A CTFM version using a hybrid stator, made of a combination of SMC and Fe-Si laminations or amorphous material is presented in [4][6]. Compared to CTFMs made of SMC only, this configuration offers reduced iron losses while further improving its manufacturing. This paper deals with such a CTFM structure. An exploded view of one phase of a 20 pole pairs CTFM with hybrid stator is shown in Fig. 1.

Many reports of TFM design methods can be found in the literature: [2][3][5][7][8][10]. Many of them insist on the complexity of modeling and optimizing such machines. High power and torque densities of TFMs are usually obtained with a large number of poles and high electric loadings. This unfortunately implies that optimized TFM designs are penalized by an inherent poor magnetic coupling (high leakage fluxes) which translates into low power factors [2][3][5]. As noted by Dickinson *et al.* in [5], the key to adequate TFM design is to minimize such unwanted leakage fluxes without reducing the mutual coupling between stator and rotor fluxes while keeping a high number of poles. Therefore, leakage paths are crucial and cannot be neglected while designing a TFM. Unfortunately, 3D flux line patterns in the machine magnetic circuit, complex leakage paths and saturation of the magnetic material significantly complicates torque prediction of CTFM and TFM in general.

For these reasons, finite element (FE) simulations are commonly used in the design process [2][3] [10]. The 3D structure of the CTFM requires heavy time-consuming finite element analyses (FEA) that are not well suited to iterative optimization procedures. Therefore, CTFM design processes based on FEA often rely on simple cut and try experimentations guided by the designer's knowledge [3] [10]. It is the author's experience that such a design approach is time-consuming but also frustrating as there is no guarantee of convergence towards one true optimal solution.

Analytical models are, in general, preferable to FEA simulations for the design and optimization processes as they are faster to solve and enable better exploration of the solution space. In [2][10], simplified magnetic reluctance networks are used to derive CTFM fluxes and calculate the machine torque. However, these magnetic models neglect leakage paths and saturation, eventually leading to significant prediction errors , thus restraining their use to estimate initial values for a FEA-based optimization process. Flux and torque values can also be evaluated with rather complex magnetic reluctance networks as those presented in [5][7][8]. Such reluctance networks model 3-D flux paths in the CTFM magnetic circuit and leakage paths as well through several reluctances. This is also the direction chosen in this paper. In [8][9], flux paths and reluctance expressions are derived by averaging the output of a very large number of FEA simulations, which is a substantial computational burden, with no guarantee of reaching acceptable accuracy, as pointed out in [9]. In addition, [7][8] also take into account the non-linear characteristics of ferromagnetic materials. Despite their complexity, such

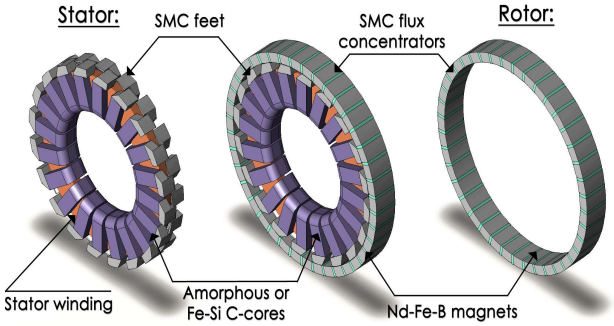

Fig. 1. 1 phase, 20 pole pairs CTFM with hybrid stator. Left: stator. Center: whole motor phase. Right: rotor.

N. Dehlinger and M. Dubois are with the Laboratoire d'Électrotechnique, d'Électronique de Puissance et de Commande Industrielle (LEEPCI)Département de Génie Électrique et d'Informatique, Université Laval, Québec, Canada (e-mail: nicolas.dehlinger.1@ulaval.ca).

models can rather easily be programmed to be employed in an optimization procedure as in [5]. It is the author's experience that the accuracy of such complex reluctance models is rather dependent on the machine dimensions: assumptions taken to model main and leakage paths are strongly related to the magnetic circuit shape and dimensions. While accurate for some machine designs, it can lead to significant errors for others. Using similar models, Dubois reports errors between analytical and FE results varying between -3 % and 25 % on flux estimations with 10 different TFM designs [9].

This paper addresses the difficulty of modeling and optimizing TFMs by presenting the basis of a new and original design method applied to the CTFM with hybrid stator structure. The method uses a magnetic model, expressed as a comprehensive reluctance network, which models both machine main flux path and leakage flux paths. This work is the subject of a companion paper [11], where this model is found to be very accurate for any machine design because it is equipped with an error compensation mechanism. It is shown in [11] how FEA-derived correction factors applied to selected reluctances guarantee the validity of the model results during an optimization process. In the remainder of the current paper, the model is briefly recalled, along with the compensation mechanism detailed in [11]. Moreover, TFM machine optimization with correction factors will be investigated in more depth, as a natural complement to the modeling method covered in the companion paper.

As in [11], this study is limited to the no-load case: the model presented in this paper allows the accurate calculation of the no-load flux of a CTFM with hybrid stator within a design process along with the design optimization of such a machine, where the no-load flux needs to be maximized. Maximization of no-load flux is of critical importance in TFM machines, for the sake of increasing the machine power factor as much as possible. Regarding the maximization of the machine torque, a machine with high no-load flux will also greatly contribute enhance the machine torque, although the armature flux contribution should also be considered. Further works are still required to develop a model that maximizes torque, considering the armature flux as well as the no-load flux. This will not be the subject of this paper, as the present discussion focuses on the optimization of the machine design parameters with respect to the maximization of no-load flux

II. Analytical Model Used for the Determination of the Machine No-Load Flux Linkage

This section intends to introduce the proposed CTFM reluctance model and the error compensation mechanism, which has been described more extensively in [11]. The CTFM no-load flux is calculated from an analytical procedure based on a magnetic reluctance network. The determination of the main flux path and the leakage flux paths was addressed from an accurate observation of the flux

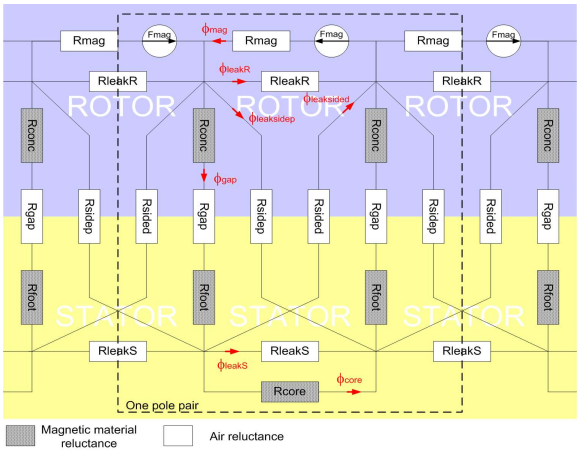

Fig. 2. Equivalent magnetic reluctance network used for the determination of the CTFM no-load flux-linkage.

patterns in a typical 3D FEA. Whenever the reluctance model is found to be inadequate, the errors are compensated with correction factors applied to selected reluctances. In addition, material non-linearities are also taken into account in the model.

A. Reluctance network and no-load-flux expression

Fig. 2 shows the reluctance network considered here. Using the motor symmetry, this network is reduced to one pole pair. R_{conc}, R_{foot} and R_{core} are the reluctances respectively associated to the machine rotor concentrator, stator foot and core. R_{mag} represents the magnet reluctance. R_{gap} is the airgap reluctance under a half rotor pole. R_{leakR} and R_{leakS} are the reluctances respectively associated to flux leakage paths between adjacent rotor PMs and the stator feet. R_{sided} and R_{sidep} represent the leakage reluctances between the stator feet and rotor concentrators from both sides of a foot. F_{mag} is associated to the PM magnetomotive force (MMF). Analytical expressions for the reluctances depicted in Fig. 1 have been determined from the motor geometrical dimensions and material characteristics. These expressions as well as the assumptions made are detailed in the companion paper [11]. Applying Kirchhoff's laws to the reluctance network gives the following system of equations:

$$\begin{cases} 2\cdot(\phi_{mag}-\phi_{leakR})-\phi_{leaksided}-\phi_{leaksidep}-\phi_{gap}=0 \\ 2\cdot(\phi_{mag}-\phi_{leakR}-\phi_{leaksided}-\phi_{leaksidep}-\phi_{leakS})-\phi_{core}=0 \\ F_{mag}-R_{mag}\cdot\phi_{mag}-R_{leakR}\cdot\phi_{leakR}=0 \\ F_{mag}-R_{mag}\cdot\phi_{mag}-2\cdot(R_{conc}+R_{gap}+R_{foot})\cdot\phi_{gap}-R_{core}\cdot\phi_{core}=0 \\ F_{mag}-R_{mag}\cdot\phi_{mag}-(R_{conc}+R_{gap}+R_{foot})\cdot\phi_{gap}-R_{sided}\cdot\phi_{leaksided}=0 \\ F_{mag}-R_{mag}\cdot\phi_{mag}-(R_{conc}+R_{gap}+R_{foot})\cdot\phi_{gap}-R_{sidep}\cdot\phi_{leaksidep}=0 \\ R_{leakS}\cdot\phi_{leakS}-R_{core}\cdot\phi_{core}=0 \end{cases} \quad \text{(I)}$$

ϕ_{mag}, ϕ_{leakR}, ϕ_{gap}, $\phi_{leaksided}$, $\phi_{leaksidep}$, ϕ_{leakS}, ϕ_{Core} represent the branch fluxes (per pole pair) of the reluctance network, ϕ_{Core} being the machine no-load flux (per pole pair). As explained in [11], a mathematical software has been used to determine analytical expressions for each of the 7 branch fluxes of system (I). The resulting expression for the no-load flux ϕ_{Core} (per pole pair) is described by Eq. (2).

$$\phi_{core}=-(2\cdot F_{mag}\cdot R_{leakR}\cdot R_{leakS}\cdot(R_{gap}\cdot R_{sided}+R_{gap}\cdot R_{sidep}-R_{sided}\cdot R_{sidep}+R_{conc}\cdot(R_{sided}+R_{sidep})+R_{foot}\cdot(R_{sided}+R_{sidep})))/(2\cdot R_{leakR}\cdot(2\cdot(R_{foot}+R_{gap})\cdot R_{leakS}\cdot R_{sided}\cdot R_{sidep}+R_{conc}\cdot(2\cdot R_{leakS}\cdot R_{sided}\cdot R_{sidep}+R_{core}\cdot(4\cdot R_{sided}\cdot R_{sidep}+R_{leakS}\cdot(R_{sided}+R_{sidep})))+R_{core}\cdot(R_{leakS}\cdot R_{sided}\cdot R_{sidep}+R_{foot}\cdot(4\cdot R_{sided}\cdot R_{sidep}+R_{leakS}\cdot(R_{sided}+R_{sidep}))+R_{gap}\cdot(4\cdot R_{sided}\cdot R_{sidep}+R_{leakS}\cdot(R_{sided}+R_{sidep}))))+R_{mag}\cdot(R_{leakS}\cdot(R_{leakR}\cdot R_{sided}\cdot R_{sidep}+R_{foot}\cdot(4\cdot R_{sided}\cdot R_{sidep}+R_{leakR}\cdot(R_{sided}+R_{sidep}))+R_{gap}\cdot(4\cdot R_{sided}\cdot R_{sidep}+R_{leakR}\cdot(R_{sided}+R_{sidep})))+R_{conc}\cdot(R_{leakS}\cdot(4\cdot R_{sided}\cdot R_{sidep}+R_{leakR}\cdot(R_{sided}+R_{sidep}))+2\cdot R_{core}\cdot(4\cdot R_{sided}\cdot R_{sidep}+R_{leakR}\cdot(R_{sided}+R_{sidep})+R_{leakS}\cdot(R_{sided}+R_{sidep})))+2\cdot R_{core}\cdot(R_{leakR}\cdot R_{leakS}\cdot R_{sided}+R_{leakR}\cdot R_{leakS}\cdot R_{sidep}+R_{leakR}\cdot R_{sided}\cdot R_{sidep}+R_{leakS}\cdot R_{sided}\cdot R_{sidep}+R_{foot}\cdot(4\cdot R_{sided}\cdot R_{sidep}+R_{leakR}\cdot(R_{sided}+R_{sidep})+R_{leakS}\cdot(R_{sided}+R_{sidep}))+R_{gap}\cdot(4\cdot R_{sided}\cdot R_{sidep}+R_{leakR}\cdot(R_{sided}+R_{sidep})+R_{leakS}\cdot(R_{sided}+R_{sidep}))))) \quad \text{(2)}$$

B. Material saturation concerns

R_{conc}, R_{foot} and R_{core} (darkened in Fig. 1) are affected by saturation as they represent flux paths through the motor soft-magnetic parts. Non-linearities of the magnetic materials are considered in the analytical model by adjusting the material permeability according to their B-H curves. Non-linear permeabilities μ_{conc}, μ_{foot} and μ_{core} are considered respectively in R_{conc}, R_{foot} and R_{core} expressions. The latter are calculated using a numerical procedure involving a non-linear system solver (which does not involve FEA) which iteratively uses the core flux calculated with the analytical model in order and determines the permeability to be used from the value of B obtained analytically and the material B-H curves. Considering non-linear permeabilities of the machine magnetic circuit materials, the expression of ϕ_{Core} (Eq. 2) enables calculating the saturated no-load flux.

C. Error compensation mechanism

The model accuracy is dependent on the motor's magnetic circuit dimensions as shown in [11]. While accurate for some designs, significant differences between the results obtained with the model and FEA have also been observed. Errors on the analytical no-load flux estimation varying between -16% and 10 % have been observed considering 4 different CTFM designs [11]. The difficulty in obtaining accurate magnetic models for TFM has also been noted by several authors in the literature as pointed in [2][5][7]-[10]. Such inaccuracies prevent the current model to be used in an optimization process, as it could lead to false optimal designs. A solution to this problem has been presented in [11]: this is done by equipping the analytical model with an error compensation mechanism. Correction factors are applied to selected reluctances of the model during the design process. As pointed in the literature [7]-[10] and in the companion paper [11], errors mainly occur in predicting flux leakage and flux path in the airgap. Therefore, 5 correction factors, k_{leakR}, k_{leakS}, k_{sided}, k_{sidep} and k_{gap} are applied to the leakage reluctances R_{leakR}, R_{leakS}, R_{sided}, R_{sidep} as well as the airgap reluctance R_{gap}. The resulting corrected model is used inside an optimization loop. Once an optimal design has been found, the model results have to be validated and its correction factors values changed if necessary. For each intermediate optimal design found after an optimization, one compares the fluxes calculated analytically from the reluctance model to those obtained by a 3D FE computation. Whenever a difference exists between the fluxes, corrections factors values are adjusted by a least-square method aimed to minimize the differences. Results have shown that the method is rather efficient reducing model errors to negligible levels [11].

The error compensation method combined to the developed reluctance model is destined to be used within a CTFM design process. As an analytical model is used inside the optimization loop, the optimization process itself is rather fast. Moreover, the use of the error compensation mechanism ensures a sufficient accuracy to the analytical model. This method provides optimal solutions whose validity is guaranteed by a limited number of FE simulations. The following section presents an example of CTFM optimization using this method.

III. CTFM No-Load Flux Optimization

The reluctance model and the error compensation mechanism presented in the previous section are now used in an optimization context. This section shows the effectiveness of this CTFM design methodology. For this purpose, a case of study of CTFM no-load flux maximization is presented. The optimality of design solutions provided this optimization methodology is also discussed.

A. Optimization principles

The analytical model described of Fig.1 has been implemented in a Microsoft Excel® worksheet. The no-load flux equation (Eq. (2)) as well as the expressions of the 6 other branch fluxes have also been inserted in the worksheet thus giving direct relations between the machine dimensions and magnetic performances. Flux calculations considering non-linear material characteristics are achieved using algorithms developed in Visual Basic macros. The compensation error mechanism has been implemented in the worksheet. Visual Basic macros have been developed to link worksheet data to the FE software Infolytica® Magnet VI® in order to build, simulate and get results from FE models to determine the correction factors. Using Microsoft Excel®'s solver, the developed worksheet acts as a simple and powerful CTFM design tool. The main dimensions of one CTFM pole pair are identified in Fig. 3. The optimization procedure presented in this paper consists in finding optimal sets of machine geometrical dimensions maximizing the no-load flux. The optimization variables of the machine consist in 8 geometrical form factors, in connection with the CTFM geometry. Expressions of the 8 form factors k_{smag}, k_{rot}, k_{ap}, k_{cp}, k_{rp}, k_{hb}, k_{hp} *and* k_{pn} are:

$$k_{smag} = L_a/H_a = magnet\ thickness/magn\quad height$$
$$k_{rot} = L_a/L_c = magnet\ thickness/concentrator\ thickness$$
$$k_{ap} = H_{gp}/H_a = to\quad foot\ height/magnet\ height$$
$$k_{cp} = L_{pp}/L_c = foot\ airgap\ thickness/concentrato\ \ thickness$$
$$k_{rp} = P_{gp}/P_r = foot\ airgap\ depth/concentrato\ \ depth$$
$$k_{hb} = H_{bp}/H_{gp} = fo\quad height\ near\ the\ airgap/total\ foot\ height$$
$$k_{hp} = H_{pp}/H_{gp} = foot\ height\ near\ the\ core/total\ foot\ height$$
$$k_{pn} = L_n/L_{pp} = core\ thickness/foot\ airgap\ thicknes$$

5 other dimensions, such as the rotor external diameter R_a, the airgap length e, the machine depth P_r, the pole pair number p and the winding area A_{bob} have been set as fixed, input parameters of the optimization problem. Several geometrical constraints are also considered to ensure that every design is physical (ex: $0 < k_{smag} < 1$). The optimization process (Fig. 4), can be summed to the following 4 steps:

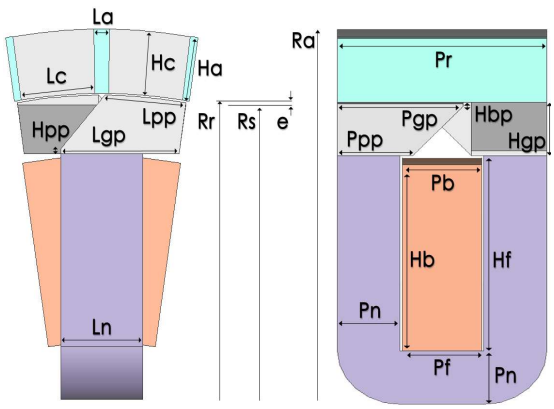

Fig. 3. Main dimensions and variables used for the design.

- ***Step 1:*** Inside the optimization loop, the reluctance model of section II is used to determine the motor saturated no-load flux (Eq. (2)) as well as the other 6 branch fluxes, from an initial set of input (R_a, e, P_r, p and A_{bob}) parameters and from optimization parameters (k_{smag}, k_{rot}, k_{ap}, k_{cp}, k_{rp}, k_{hb}, k_{hp} k_{pn}).
- ***Step 2:*** A temporary solution is then found with Excel's solver which maximizes the no-load flux with an initial set of values for the correction factors.
- ***Step 3:*** A 3D FE simulation is performed considering the machine geometrical parameters of this temporary solution. The output of this step is the computation of the main flux and leakage fluxes with the FE software.
- ***Step 4:*** The 5 correction factors, k_{leakR}, k_{leakS}, k_{sided}, k_{sidep} and k_{gap} applied to the reluctances R_{leakR}, R_{leakS}, R_{sided}, R_{sidep} and R_{gap} are modified in order to compensate the errors in the analytical model.

These 4 steps (1-2-3-4) are then started with the new values for the correction factors. The whole process is repeated until negligible errors are found between the fluxes calculated with the model and those computed from 3D-FE, giving a final, optimized set of geometrical parameters, which maximize the no-load flux in the machine, for a given set of input values (R_a, e, P_r, p and A_{bob}).

B. CTFM optimization example

Fig. 5 presents an illustration of one pole pair of a non-optimized CTFM as well as its main dimensions as an arbitrary starting point. The latter have been selected for the purpose of this example. The design process described in this paper has been applied to this particular machine: the values of k_{smag}, k_{rot}, k_{ap}, k_{cp}, k_{rp}, k_{hb}, k_{hp} and k_{pn} in Fig. 5 have been considered as initial values of the optimization. Following the procedure shown on Fig. 4, an optimal set of these 8 parameters maximizing the machine no-load flux has been found. These optimal parameters as well as an illustration of the optimized design are shown in Fig. 6.

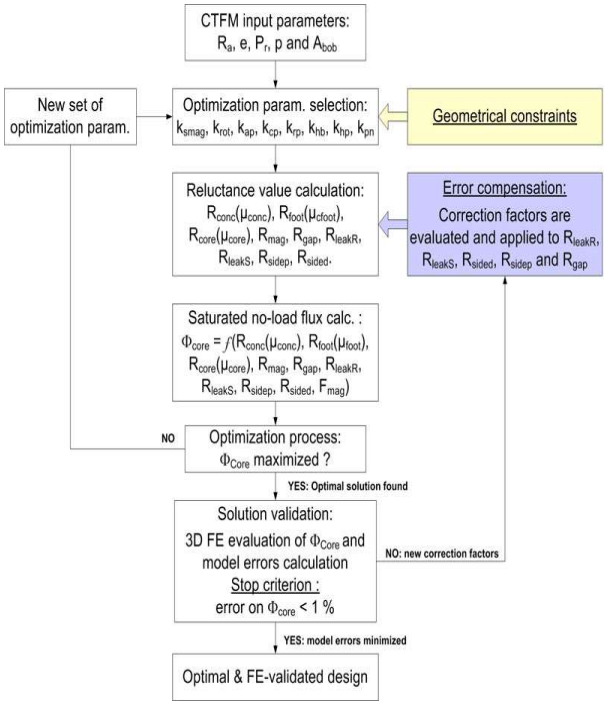

Fig. 4. Flowchart describing the optimization process employed to maximize the CTFM no-load flux

CTFM dimensions before no-load flux optimization	
R_a	1000 mm
e	0.80
P_r	100 mm
p	100
A_{bob}	5000 mm²
k_{smag}	**0.70**
k_{rot}	**0.40**
k_{ap}	**0.60**
k_{cp}	**1.10**
k_{rp}	**0.60**
k_{hb}	**0.30**
k_{hp}	**0.15**
k_{pn}	**1.5**
μ_{core}	**2870**
μ_{conc}	**205**
μ_{foot}	**154**
ϕ_{Core}	**638 µWb**

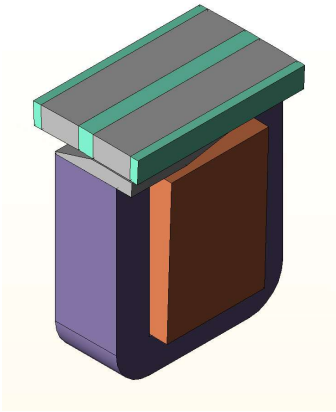

Fig. 5. Optimization and input parameters of a CTFM design before no-load flux maximization. No-load flux per pole ϕ_{Core} is given as well.

CTFM dimensions obtained after no-load flux optimization	
R_a	1000 mm
e	0.80
P_r	100 mm
p	100
A_{bob}	5000 mm²
k_{smag}	**0.13**
k_{rot}	**0.25**
k_{ap}	**0.46**
k_{cp}	**1.11**
k_{rp}	**0.76**
k_{hb}	**0.05**
k_{hp}	**0.05**
k_{pn}	**1.84**
μ_{core}	**5160**
μ_{conc}	**156**
μ_{foot}	**90**
ϕ_{Core}	**1240 µWb**

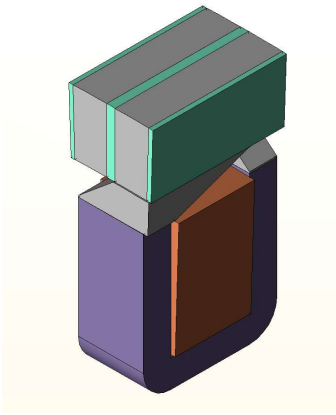

Fig. 6. Optimization and input parameters of a CTFM design obtained after no-load flux maximization. Maximized no-load flux ϕ_{Core} is given as well.

- *Optimized design dimensions and performances*

A 3-D FE simulation has been performed to evaluate the no-load flux linking the winding of the CTFM before the optimization giving a flux of 638 µWb, as shown on the table of Fig. 5,. At the end of the optimization process, the optimized design presents a value of no-load flux of 1240 µWb (ϕ_{Core} in Fig. 6). With a flux almost twice higher, this solution proves that the method substantially increases the no-load flux, as expected. Resulting relative permeabilities μ_{conc}, μ_{foot} and μ_{core} of the initial and optimal designs used in the analytical model are also given in tables of Fig. 5 and 6.

- *Variation of the optimized CTFM parameters*

Fig. 7 presents the variation of the optimized CTFM parameters k_{smag}, k_{rot}, k_{ap}, k_{cp}, k_{rp}, k_{hb}, k_{hp} and k_{pn} during the design process. One can notice that these parameters rapidly reach a constant value. Parameters k_{smag}, k_{rot}, k_{ap}, k_{cp}, k_{rp}, k_{hb} and k_{hp} only require 2 iterations to reach a constant value when k_{pn} requires 3 iterations. After 3 iterations, optimized parameters do not evolve anymore. This observation helps us to conclude that an optimal CTFM design has already been found after 3 iterations of the design process. The 2 last iterations mainly consist in finding correction factor values validating the model results as confirmed later by the observation of Fig. 8 and Fig. 9. The geometrical parameter values of the final solution are k_{smag} = 0.13, k_{rot}= 0.25, k_{ap}= 0.46, k_{cp}= 1.11, k_{rp}= 0.76, k_{hb}= 0.05, k_{hp}= 0.05 and k_{pn}= 1.84 corresponding to the values presented in the table of Fig.6.

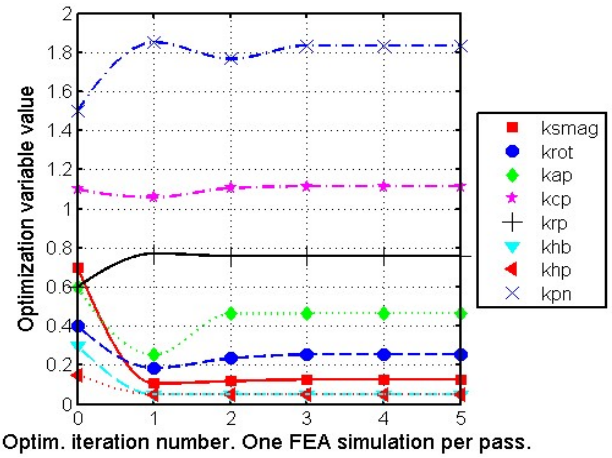

Fig. 7. Variation of the 8 optimized CTFM parameters k_{smag}, k_{rot}, k_{ap}, k_{cp}, k_{rp}, k_{hb}, k_{hp} and k_{pn} during the design process.

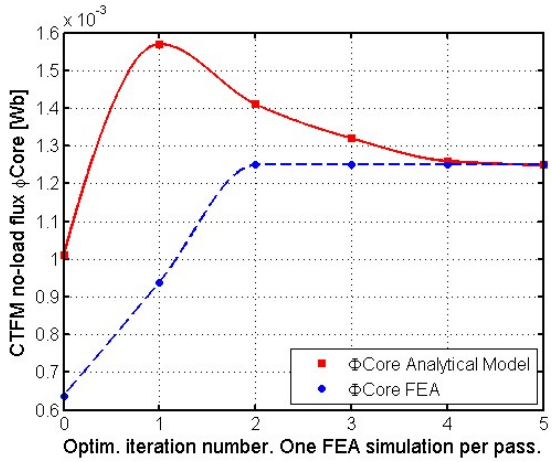

Fig. 8. Variation of the saturated no-load fluxes estimated analytically and with FEA during the whole design process.

- *Variation of the FEA and analytical model estimated no-load fluxes during the design process*

The graph presented in Fig. 8 shows the variation of the optimized no-load flux per pole ϕ_{Core} estimated with the analytical model over the whole design process. It also presents the corresponding no-load flux obtained from FEA used for validation in the error compensation process. Fig. 8 helps to better understand how the CTFM design method works. At optimization iteration #1, a first set of parameters maximizing the no-load flux has been found. A first FE simulation is then performed to validate the fluxes calculated with the model, considering the optimal parameters found. At optimization iteration #1, one can clearly notice that a huge difference exists between the no-load flux calculated analytically and the one obtained from FEA: indeed, a difference of 68 % between the 2 fluxes can be observed. Therefore, corrections factors are calculated and applied to the model to minimize the model errors. At optimization iteration #2, a new set of parameters has been found considering the correction factors calculated at the previous step. A second FE simulation is performed and it can be noticed that the difference between the analytical and FEA no-load fluxes has been reduced to 13 %. New values of correction factors are then calculated and the whole process repeats until the errors between analytical and FE results are found negligible (< 1 %). Fig. 8 shows that the whole design process converged rather quickly: 5 iterations with the FE software were sufficient to minimize the analytical model errors and to validate the optimal solution found. After 5 simulations, the no-load flux obtained analytically equals the no-load flux computed with FE

- *Variation of the model fluxes errors*

The graph presented in Fig. 9 shows the variation of the difference observed between the no-load flux ϕ_{Core} obtained with the analytical model and the same flux computed with FEA during the design process. As detailed in [1], correction factors are calculated from a least-square process minimizing the errors observed between the fluxes calculated analytically and the fluxes obtained from FEA. The graph in Fig. 9 also shows the sum of the squared errors made while estimating the 7 fluxes of the reluctance networks. Curves in Fig. 9 clearly show that the error compensation mechanism is rather efficient: after 5 iterations with the FE software, the

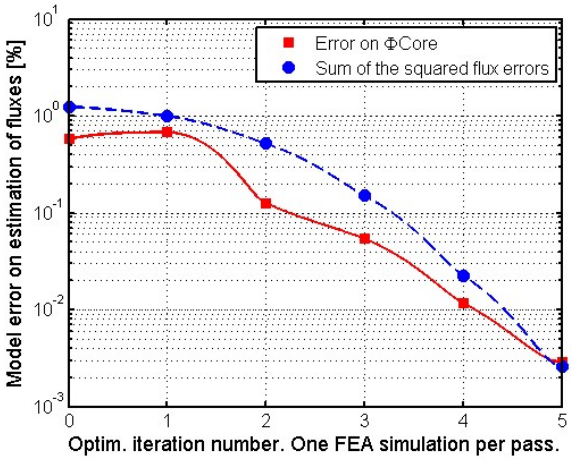

Fig. 9. Variation of squared fluxes errors and error made on the no-load flux estimated analytically during the design process. All errors correspond to the difference in % observed between model and FEA fluxes (1% = 10^{-2}).

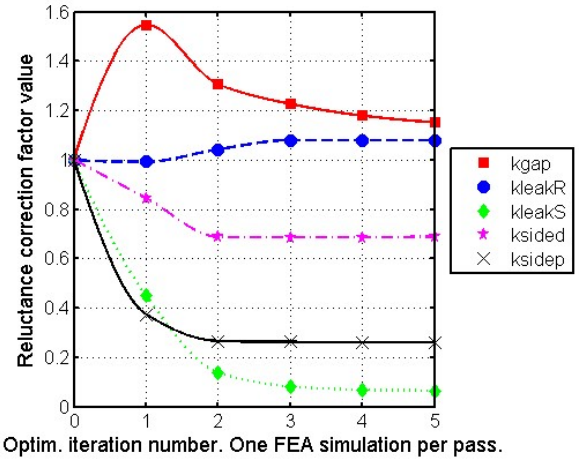

Fig. 10. Variation of the correction factors k_{gap}, k_{leakR}, k_{leakS}, k_{sided} and k_{sidep} during the design process.

sum of squared fluxes errors have been reduced to 0.0026. Similarly, the error on ϕ_{Core} went from 68 % after the first iteration and FE simulation to 0.3 % after the 5th iteration.

- *Variation of the correction factors*

During the design process, correction factors k_{gap}, k_{leakR}, k_{leakS}, k_{sided} and k_{sidep} values are adjusted by a least-square method to compensate for the model errors. Fig. 10 presents the variation of the 5 correction factors over the design process considered in this example. Initialized at 1 before the

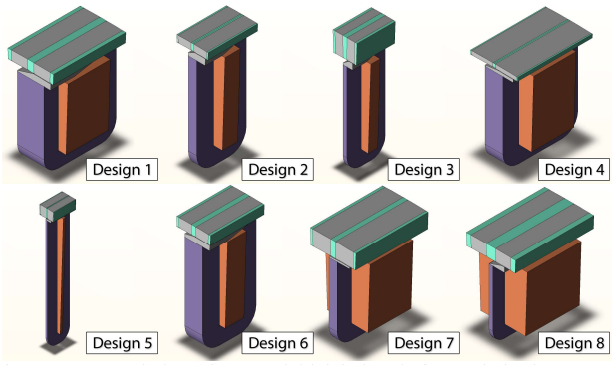

Fig. 11. 8 CTFM designs chosen as initial designs before optimization.

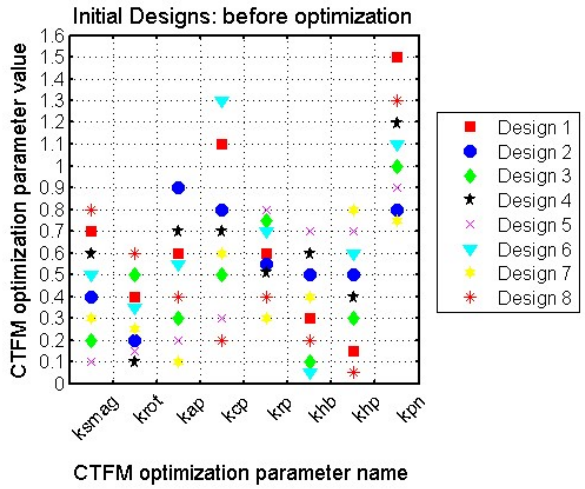

Fig. 12. CTFM parameters k_{smag}, k_{rot}, k_{ap}, k_{cp}, k_{rp}, k_{hb}, k_{hp} and k_{pn} chosen as initial values of 8 design processes.

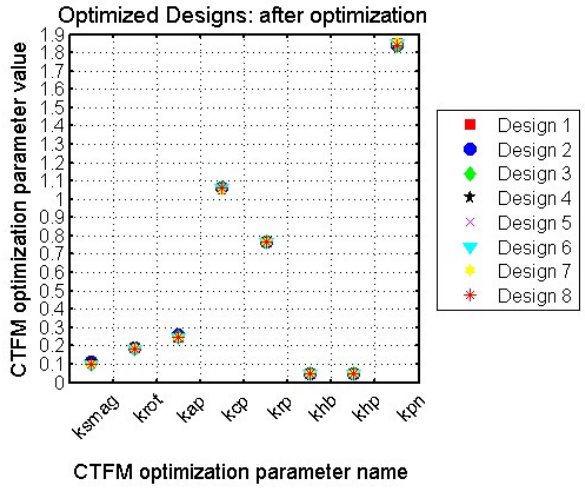

Fig. 13. CTFM optimal parameters k_{smag}, k_{rot}, k_{ap}, k_{cp}, k_{rp}, k_{hb}, k_{hp} and k_{pn} of 8 designs found after no-load flux maximization before error compensation.

process, their values change rapidly after the first FE simulations. After 2 iterations only, factors k_{sided} and k_{sidep} have already reached their final value respectively at 0.69 and 0.26 for the design considered here. However, one can notice that factors k_{gap}, k_{leakR} and k_{leakS} need 5 iterations before stabilizing. In the design example considered in this section, final values for correction factors k_{gap}, k_{leakR}, k_{leakS}, k_{sided} and k_{sidep} are respectively 1.15, 1.08, 0.06, 0.69 and 0.26.

- *Design method computation time*

With the example considered here, 5 optimization iterations were required for a total of 5 FE simulations. It is the author's experience that 4 to 6 iterations are generally sufficient for a whole CTFM design process. The time required for the maximization of a CTFM no-load flux mostly depends on the number of FE simulations required, the FE mesh settings but also the size of the CTFM. For FE simulations, a particular attention is paid to refine the mesh in airgap and leakage regions for sufficient accuracy. In the example presented here, a mesh containing more than 730000 elements has been considered. Run on a 2.61 GHz Athlon® processor, each FE simulation requires almost 15 minutes. The analytical determination of the saturated no-load flux as well as the optimization do not require more than 1 minute per pass. Therefore, the design process total duration for the example considered here is about 80 minutes. Such a computation time is rather low if one considers that the method provides an optimal FE-validated CTFM design solution.

- *Optimality of the solutions obtained*

The question of the optimality of the solutions obtained with the method described in this paper should be addressed. In other words, it must be verified if the optimization method and the analytical model are efficient enough to avoid convergence to local optimum in the solution space. As there is no evident mathematical way to prove this, a more practical approach has been followed.

8 different CTFM optimization parameter sets (k_{smag}, k_{rot}, k_{ap}, k_{cp}, k_{rp}, k_{hb}, k_{hp} and k_{pn}) have been selected as initial parameters for 8 design processes. R_a = 1000 mm, e = 0.8 mm, P_r = 100 mm, p =100 and A_{bob} = 5000 mm², have been chosen as fixed input parameters. These latter are similar as those of the design example previously described (see tables in Fig. 5 and Fig. 6.). The 8 initial optimization parameters sets have been selected in order to cover a wide space of solutions during optimizations: they represent 8 CTFM designs with different shapes and dimensions. Fig. 11 presents illustrations of these 8 initial designs. Fig. 12 shows a graph representing their corresponding 8 initial optimization parameters sets (Design 1 to Design 8).

A part of the optimization method of this paper has been applied to the 8 initial CTFM designs with the parameters presented in Fig. 12. The analytical procedure described above has been used to determine 8 optimal sets of parameters (k_{smag}, k_{rot}, k_{ap}, k_{cp}, k_{rp}, k_{hb}, k_{hp} and k_{pn}) maximizing the saturated no-load flux starting with the 8 initial designs. Same optimization constraints have been adopted for the 8 optimization problems.

The corresponding 8 optimal sets of parameters after the no-load flux maximization are shown in Fig. 13 (Design 1 to Design 8). One can notice that the 8 optimization problems nearly converged to the same solution: the same parameter set (k_{smag} = 0.11, k_{rot}= 0.19, k_{ap}= 0.25, k_{cp}= 1.06, k_{rp}= 0.77, k_{hb}= 0.05, k_{hp}= 0.05 and k_{pn}= 1.84) has been found as the optimal set maximizing the no-load flux starting from 8 different initial parameter sets. Only small biases are observed between the designs: for example, the optimal value of k_{smag} has been found equal to 0.11 for Design 1 while it converged to 0.10 for Design 8. The optimal parameters set found corresponds to the one obtained with the model at FEA iteration #1 in Fig. 7 before the first error compensation. As the same optimal parameter set has been found since the first design step for the 8 designs, it is

expected that similar correction factors will be obtained during the design process. Similarly, same final optimal parameters are expected at the end of the design process in the 8 cases. It is therefore not necessary to continue the design process until FEA iteration #5. As this observation does not constitute a proper mathematical proof, it still provides us good confidence on the optimality of the solutions found with the design method.

IV. Conclusion

In this paper, we introduced an approach to address the challenge of modeling and optimizing TFMs. A new design method is presented and applied to maximize the no-load flux of a CTFM with hybrid stator. An error compensation mechanism combined to an analytical reluctance model is proposed as a solution to overcome inherent inaccuracies of TFM analytical models.

After a brief introduction on the model along with the compensation mechanism described in a previous communication [11], optimization aspects of the design method have been presented. A case of study of CTFM no-load flux maximization has been investigated. The method has been used to find an optimal set of geometrical parameters considering one particular CTFM design. It has been found that only 5 iterations with the FE software were required to compensate for the analytical model errors and validate the optimal solution found. After optimization, a 100 % increase in no-load flux has been observed. Variations of the correction factors and model errors during the optimization process have been presented as well. Finally, the optimality of the solutions found with this method has been discussed. Optimization results obtained gave us good confidence about the convergence and the optimality of the solution found using this method.

Ongoing works are now focused on developing the model and adapting the design method for CTFM armature flux and torque prediction. Even if the method presented in this paper has been applied to the CTFM topology, a similar approach could also be considered for the design of other TFM configurations or machines for which it is difficult to derive analytical models.

V. References

[1] Weh H., May H., "Achievable Force Densities for PM Excited Machines in New Configurations", in *Int. Conf. on Elec. Mach. - ICEM, pp. 1107-1111, Sept. 1986, München, Germany.*

[2] Viorel I.-A., Henneberger G., Blissenbach R., Löwenstein L., "Transverse Flux Machines. Their Behaviour, Design, Control and Applications", *Mediamira 2003, Cluj, Romania.*

[3] Maddison C.P., Mecrow B.C. and Jack A.G, "Claw Pole Geometries For High Performance Transverse Flux Machines", *Int. Conf. on Elec. Mach. ICEM, pp. 340-345, Sept. 98, Vigo, Spain.*

[4] Dubois M.R., Dehlinger N., Polinder H., Massicotte D., "Clawpole Transverse Flux Machine with Hybrid Stator", in *Int. Conf. on Elec. Mach. - ICEM, paper 412, Sept. 2006, Chania, Greece.*

[5] Dickinson P.G., Jack A.G., Mecrow B.C., "Improved Permanent Magnet Machines with Claw Pole Armatures", in *Int. Conf. on Elec. Mach. - ICEM, pp. 1-5,Aug. 2002, Bruges, Belgium.*

[6] Dehlinger N., Dubois M.R., "Clawpole Transverse Flux Machine with Amorphous Stator Cores", in *Int. Conf. on Elec. Mach. - ICEM, paper 1017, Sept. 2008, Vilamoura, Portugal.*

[7] Ibala A., Masmoudi A., Atkinson G., Jack A.G. , "A New Reluctance Model of a Claw Pole TFPM using SMC for the Magnetic Circuit", in *Int. Conf. on Eco. Vehic. and Ren. Ener. -EVER, March 2009, Monte Carlo, Monaco.*

[8] Ibala A., Masmoudi A., Atkinson G., Jack A.G. , "Investigation of the Leakage Fluxes of SMC Made Magnetic Circuit Claw Pole TFPM", in *Int. Conf. on Eco. Vehic. and Ren. Ener. -EVER, March 2009, Monte Carlo, Monaco.*

[9] Dubois M.R.., "Optimized Permanent Magnet Generator Topologies for Direct-Drive Wind Turbines", *PhD Thesis, Delft University of Technology, Delft, The Netherland, 2004.*

[10] Blissenbach R., "Entwicklung von Permanenterregten Transversalflussmaschinen hoher Drehmomentdiche für Traktionsantriebe", *PhD Thesis, RWTH Aachen, Oct. 2002, Aachen, Germany* [In German].

[11] Dehlinger N., Dubois M.R., "A New Design Method for the Clawpole Transverse Flux Machine. Application to the Machine No-Load Flux optimization. Part I: Accurate Magnetic Model with Error Compensation.", in *Int. Conf. on Elec. Mach. - ICEM, Sept. 2010, Rome, Italy.*

VI. Biographies

Nicolas Dehlinger was born in Sarreguemines, France. He received the engineering degree from the Université de Technologie de Belfort-Montbeliard (UTBM), France, in 2005 and the MSc degree from Université Laval, Canada, in 2007. He is currently working towards a PhD degree in the research laboratory LEEPCI from Université Laval. Since 2010, he also works as an electrical design engineer for Alstom Hydro in Canada. His main interests are electrical machine modeling and optimization.

Maxime Dubois obtained his Bsc and MSc in Electrical Engineering from the Université Laval, in 1991 and 1993. Between 1993 and 1999 he has worked in the industry as an electronic designer. He obtaineda PhD cum laude from Delft University of Technology in The Netherlands in 2004. Since 2004, he has been Associate Professor at the department of Electrical & Computer Engineering at the Université Laval. His interests are the electromechanical conversion, the optimization of electrical machines, the design of magnetic actuators and power electronics applied mainly to the field of wind energy and electric vehicles. Mr. Dubois is the founder of several companies in the area of energy management.